Investigation of the Load-settlement Behavior of Box-shaped Deep Foundations

Serdar Günay[1*], Özer Çinicioğlu[1]

[1] Department of Civil Engineering, Faculty of Engineering, Bogazici University, 34342 Bebek Istanbul, Türkiye
* Corresponding author, e-mail: serdar.gunay@boun.edu.tr

Abstract

The load-settlement and monolithic behaviors of a new type of deep foundation in sand named Box-Shaped Deep Foundation (BSDF) were studied, and a comparison to Conventional Piled Raft Foundations (CPRF) was made by carrying out extensive numerical analysis. Physical model tests were also conducted to validate the numerical approach presented in this study, and it turned out to be a reasonable agreement. In the scope of this paper, the results of the parametric study are presented, and design strategies for an optimized design of BSDFs are discussed.

Keywords

deep foundations, box-shaped deep foundation, load-settlement behavior, numerical analysis, experimental method

1 Introduction

A box-shaped deep foundation is a new type of deep foundation, including a raft structurally connected to peripheral walls that enclose the soil. In some applications, they are sometimes called rectangular closed diaphragm walls, lattice-shaped diaphragm walls, and structural cell foundations [1–7]. BSDFs have proven appropriate for transferring structural loads into the soil and reducing excessive settlements. As a result, they have undergone substantial development worldwide as bridge foundations. Nevertheless, research on this topic is scarce, and their efficiency for other types of structures has yet to be studied deeper.

The walls and the raft form a box that physically acts as an upside-down pot. The walls under the raft are expected to constitute a frame restraining lateral movement. This frame can be square, rectangular, circular, or any shape with single or multiple cells. Around the circumference of BSDFs, sheet piles, diaphragm walls, or drilled piles may be chosen to obtain an enclosed structure. The sheet piles hold a lateral resistance but fail to transfer the vertical loads. However, diaphragm walls or bored piles could significantly increase the bearing capacity and hold a lateral resistance. In the case of a tangent pile installation, the gaps between the piles need to be strengthened by jet-grouting to ensure a closed frame. On the other hand, diaphragm walls ensure a better transfer of shear forces than bored piles do; however, the pile walls have higher skin friction.

The behavior of BSDFs has been investigated by several researchers utilizing both physical and numerical models. Brandl [1, 3] have studied the behavior of BSDFs and published a few studies. They have also named the BSDF concept an Austrian type of deep foundation. Some experimental tests have been conducted to observe the load-settlement behavior of model piles forming BSDFs. On the other hand, they have not considered the effects of soil type and soil-structure interaction. In contrast to Austrian researchers, who mostly deal with piles, some other researchers have studied the diaphragm walls as enclosing structures for the BSDF concept by referring to them as rectangular closed diaphragm wall (RCDW) and lattice-shaped diaphragm wall (LSDW) [4–7].

Some other pot-shaped foundations in the literature might be listed as skirted foundations, suction caissons, bucket foundations, and mudmat foundations [8–12]. Unlike BSDFs, skirted foundations, mostly referring to shallow foundations, usually have an aspect ratio (D/B) smaller than 2. However, foundations with larger values of aspect ratios typically between 2 and 8, refer to caissons embedded into the soil under their weight as precast structures and are mostly used for offshore structures.

The work presented herein differs from previous studies that dealt with vertically loaded BSDFs in five main aspects:

(i) Bringing all pot-shaped deep foundations with different names together under the name of BSDFs and revealing common adoption.

(ii) Including BSDFs with aspect ratios higher than 2, up to 5, which represents deep foundations and punching shear failure mode in a better way.

(iii) Introducing two new coefficients named MBR and MSR by comparing bearing capacities and settlements of BSDFs with those of embedded foundations to observe the monolithic behavior.

(iv) Introducing BCR and SRR coefficients for different geometry of BSDFs, soil types, and interface roughness to inspect the load-settlement behavior of BSDFs.

(v) Compared to piled raft foundations, it will be attempted to answer how efficient BSDFs are and in which cases they can be an alternative to conventional piled raft foundations.

This study investigates the behavior of BSDFs under vertical static loads by conducting a comprehensive numerical analysis using a 3D FEM. For this purpose, 339 numerical simulations have been performed to observe the load-settlement and monolithic behavior of BSDFs with different geometry, soil-structure interface roughness, and soil types. Furthermore, a laboratory testing program was carried out to observe the load-settlement and monolithic behavior of model BSDFs and compare them with the results of numerical analysis for validation.

2 Numerical analysis
2.1 Numerical simulation
The numerical study herein examines the performance of BSDFs by a numerical method, namely 3D FEM. PLAXIS 3D V20 (2019) has been employed to model and analyze the foundation systems [13]. The load-settlement behavior of BSDFs and CPRFs on three different sand types have been investigated through a numerical study. Firstly, a model of dimensions shown in Fig. 1 with D = 20 m and B = 8 m was simulated as the representative model. Raft and wall thickness was taken as T = 1 m and t = 0.8 m, respectively. Then, different geometry of BSDFs was also simulated for comparison and interpretation.

Brinkgreve et al. [14] claimed that for a first approximation or an early design, it is better to use an advanced constitutive model such as the Hardening Soil model with small strains than a simple model. Since most soil properties are correlated to some extent, it is argued that an analysis using an advanced model with many parameters gives a better solution with reasonable accuracy for an

early design or first approximation. For this reason, the Hardening Soil model with the small strain (HSs) was selected as the constitutive model [15, 16].

The Linear Elastic model has been selected for the structural elements of parametric studies to represent the stress-strain relationship. For concrete elements, Young's modulus E, Poison's ratio v, and unit weight of the raft and the walls are taken as 30 GPa, 0.2, and 25 kPa, respectively. For aluminum plates used in laboratory tests, unit weight, Young's modulus, and Poisson's ratio are listed as 27 kPa, 70 GPa, and 0.3, respectively.

Walls and rafts have been modelled as plate elements and piles have been modelled as volume elements. Water level is far below the foundation and drained behavior was selected. External boundaries were set sufficiently remote to get the acceptable accuracy of the results. Therefore, boundary conditions for a BSDF with raft sizes of "B × B" and foundation depth "D" were decided at 5 × B or 3 × D (bigger value) distance for the horizontal direction and 3 × D distance for the vertical direction. Mesh size influences the run time and accuracy of the computations. As the size of the elements gets smaller, run time of analyses and accuracy of results increase. In this study, mesh size was selected as "fine" for the mesh generation of the models.

A finite element analysis can be broken into successive calculation phases, followed according to an order. Firstly, the initial phase in which initial stresses take place is generated. Vertical stresses are in equilibrium with the self-weight of the volume in this phase, and the effective horizontal stresses can be calculated by utilizing the lateral earth pressure coefficient, K^0. All the soil volumes are activated in this phase, and all the structural elements, interface elements, and loads are inactivated (Fig. 2). In Phase 1, all diaphragm wall plates and relevant interface
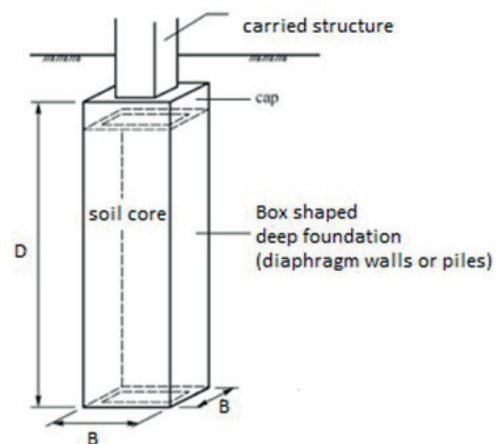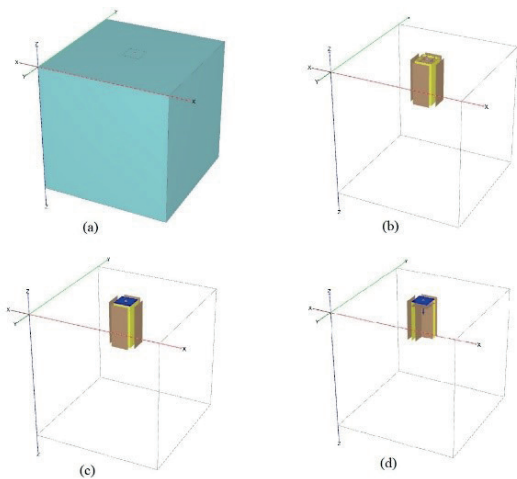

Fig. 1 3D view of a box-shaped deep foundation

Fig. 2 (a) Initial phase (b) Phase 1-Installation of the walls (c) Phase 2-Installation of the raft (d) Phase 3-Loading the BSDF

elements are activated. However, the raft and loads or displacements are still inactivated. It is important to note that the installation process of the BSDF is not simulated and assumed that installation effects if any, have only a limited impact on the mechanical behavior. In Phase 2, all diaphragm walls, raft, and relevant interface elements are activated, and loads or displacements are still inactivated. In Phase 3, the displacement control method is used, and a prescribed point displacement equal to a settlement ratio (s/B) of 20% has been carried out. Finally, it is worth stating that a plastic calculation has been conducted to calculate the load-settlement behavior of BSDFs. Although the plastic calculation does not consider the dissipation of the water and the change of the pore pressure with time, performing a fully drained analysis in plastic calculation can evaluate the settlements in the long term. This will give an accurate enough prediction of the final situation, though the consolidation process is not analyzed explicitly.

2.2 Determination of soil properties

Soil strength properties, such as a friction angle for sands and undrained shear strength for clays, can be used for stability analysis and ultimate limit design (ULS). Considering serviceability limit design (SLS), stiffness properties are also to be known. Correlations between stiffness, strength, and index properties have been studied throughout the years. Relative density (D_r) is the main index property for sands to determine strength and stiffness parameters, whereas for clays many correlations exist with the plasticity index. The relative density (D_r) is mostly given as a percentage and described as ($e_{max}-e$)/ ($e_{max}-e_{min}$), where e is the initial void ratio, e_{max} is the maximum or loosest packing void ratio and e_{min} is the minimum or densest packing void ratio.

Brinkgreve et al. [14] have suggested empirical formulas for sand to derive the model parameters for drained condition of the HSs model based on the relative density. The empirical formulas have been derived by regression analysis on a collection of soil data belonging to the general soil data, triaxial test data, and oedometer test data from previous studies. The formulas were validated by comparing them to the real test data and applying them to real cases to predict the deformations (Fig. 3, Table 1).

In this analysis, constitutive model parameters for sands with different relative densities ($S_1 = 35\%$, $S_2 = 50\%$ and $S_3 = 65\%$) were calculated using formulas in this section.

2.3 Parametric study
2.3.1 Load-settlement behavior of BSDFs

A model of dimensions with $D = 20$ m, $B = 8$ m, $t = 0.8$ m, and $T = 1$ m was first simulated as the representative model. Then, 129 different models were also simulated for comparison and interpretation. Vesić [17] demonstrated many foundations fail in the settlement ratio(s/B) of less than 10%, but in the case of the loose to medium one, the
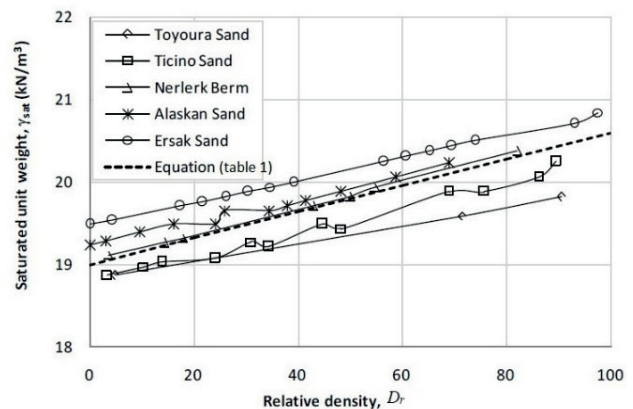

Fig. 3 Comparison of formula for saturated unit weight

Table 1 Empirical formulas for HSs model

Parameter	Formula	Unit
γ_{unsat}	$15 + 4(D_r/100)$	[kN/m²]
γ_{sat}	$19 + 1.6(D_r/100)$	[kN/m²]
E_{50}^{ref}	$60000(D_r/100)$	[kN/m²]
E_{oed}^{ref}	$60000(D_r/100)$	[kN/m²]
E_{ur}^{ref}	$180000(D_r/100)$	[kN/m²]
G_0^{ref}	$60000 + 68000(D_r/100)$	[kN/m²]
m	$0.7 - (D_{rv}/320)$	[–]
$\gamma^{0.7}$	$(2 - D_r/100)\,10^{-4}$	[–]
ϕ'	$28 + 12.5\,(D_r/100)$	[°]
ψ	$-2 + 12.5\,(D_r/100)$	[°]
R_f	$1 - (D_r/800)$	[–]

Günay and Çinicioğlu

Period. Polytech. Civ. Eng., 67(4), pp. 960–969, 2023 | 963

ultimate load (V_{ult}) might reach a bigger ratio of up to 30%. Therefore, the bearing capacity has been calculated corresponding to the 10% of the s/B ratio in all cases.

Bearing capacity ratio (BCR) is equal to the ratio of bearing capacity of BSDFs to the bearing capacity of representative shallow foundations ($D/B = 0$). The effect of the depths of BSDFs on the BCR is shown in Fig. 4(1) for three different soils. As the aspect ratio increases, so does BCR. Bearing capacities of denser soils are higher for all aspect ratios as expected. However, the increase in BCR is higher for loose sand than medium and dense sand, regardless of depth and aspect ratio.

Settlement of shallow square footings corresponding to bearing capacity for S_1, S_2 and S_3 soil types are found, which are equal to 10% of the widths. Additionally, settlements of BSDFs are measured, corresponding to constant bearing pressures of representative shallow foundations with the same widths. Settlement reduction ratio (SRR) is equal to the ratio of settlement of the BSDF to the settlement of representative shallow foundation. The inclusion of BSDF walls significantly reduces the settlement of surface foundations for all sand types. Furthermore, SRR values are in reasonable agreement with BCR values, namely that settlement reduction inclination is higher for relatively less dense sands.

Fig. 4(3–4) illustrates that BCR values decrease and SRR values increase as the width increases. It should be considered that the bearing capacities have been calculated for settlements equal to 10% of widths for BSDFs with the same lengths but different widths. Furthermore, the bearing capacity increase and settlement reduction inclination are higher for loose sand compared to medium and dense sand for changing widths. In Fig. 4(7–8), trend lines show the general behavior of BSDFs with changing aspect ratios. Considering the data of this study, BCR values tend to increase and SRR values tend to decrease as the aspect ratio increases. However, it should be noted that the different geometries with the same aspect ratios might have different BCR and SRR values.

For considering the effect of surface roughness of the foundation models, a strength reduction factor (R_{int}) specified in the interface tab sheet of the material set in PLAXIS is to be chosen. This factor relates interface strength (wall friction and adhesion) to the soil strength (friction angle and cohesion). A rigid option represented with $R_{int} = 1$ is used when the interface should not have a reduced strength with respect to the strength in the surrounding soil [18, 19].

In general, for real soil-structure interaction, the interface is weaker and more flexible than the surrounding soil, which means that the value should be less than 1. Therefore, in this section, three different R_{int} values, which are 0.6, 0,8 and 1, have been selected to represent the soil-structure interaction. As R_{int} increases, bearing capacity and BCR increase. Furthermore, based on the obtained results, it can be concluded that the improvement in the bearing capacity values increases with the increasing surface roughness of the foundation models. However, settlements and SRR values decrease with the increasing R_{int} (Fig.4(6)).

Comparing the values of BCR and SRR simulated in this study to those reported in previous literature shows that a similar trend has been observed for different aspect ratios. Furthermore, the skirted foundations achieve better in improving bearing capacity and settlement at low relative density than those at medium or high relative density sands [9–12]. In this study, BSDFs with different aspect ratios in loose sand have also achieved better results regarding bearing capacity and settlement.

After conducting experimental tests on skirted foundations up to an aspect ratio of 2, it has been concluded that this can be attributed to the fact that there is more space for increasing the shear strength of loose soils compared with dense soils. As the relative density of sand increases, the failure mode of the foundation–soil system changes due to the confinement of the formed plastic zone of sand, and hence, more displacement is required to mobilize the shear failure plane in soil. In the case of dense sand compared with loose sand, the displacement values required to mobilize strength are not enough; then, the BCR for the loose sand is obtained to be higher than dense sand.

Fig. 4(5) illustrates that the improvement in the bearing capacity values increases with the increasing surface roughness of the foundation models. This fact has been attributed to the diaphragm walls not sufficiently contributing to load transition in the case of low interface roughness. Hence, a significant part of the uniaxial loads is assigned to the tip level, which results in a decreasing rate of bearing capacity.

2.3.2 Monolithic behavior of BSDFs

The soil volume confined within the walls is to remain constant and form a stiff core utilized as an integrated load transfer element. Due to the addition of soil core, the Behavior of BSDFs gets complicated. Two approaches have been suggested to discuss to what extent a BSDF acts as a compound body [1–3]. The monolithic approach
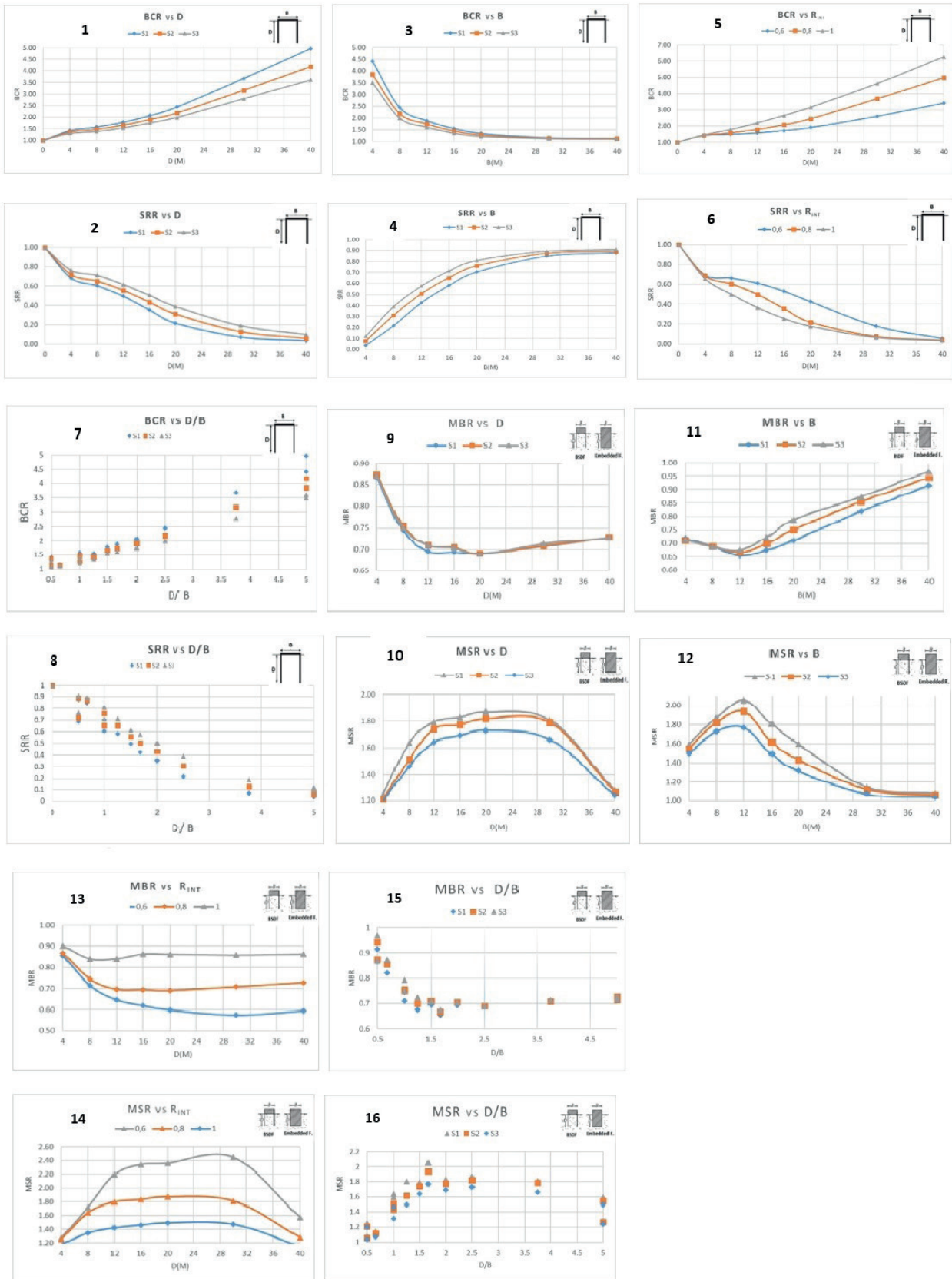
Fig. 4 BCR-SRR (1–8) and MBR-MSR (9–16) plots

represents the full composite effect between the soil core and the structural elements. The skin friction along the outside surface of the box and the bearing capacity of an equivalent shallow foundation at the bottom is used to obtain the bearing capacity of the BSDF. Secondly, in the single-element approach, skin friction is taken into consideration along the outside and inside face of the foundation. The tip resistance of piles and the bearing capacity of the raft are also calculated separately. Consequently, the actual behavior lies between these two approaches (Fig. 5).

Inspired by the two approaches, some additional cases comprising the embedded foundations have been modelled like a typical BSDF but except that their bottoms are closed, and soil cannot penetrate inside. A comparison between embedded foundations representing monolithic blocks and typical BSDFs will be made in this section. It is obvious that embedded foundations have higher bearing pressure and less settlement than BSDFs. However, the differences in bearing capacities and settlements between the two types of foundations surge as the aspect ratio rises.

Monolithic bearing ratio (MBR) is equal to the ratio of the bearing capacity of a BSDF to the bearing capacity of a representative embedded foundation. When it comes to MSR, it refers to the "monolithic settlement ratio" which is equal to the ratio of settlement of a BSDF to the settlement of an embedded foundation at the bearing pressure of a representative shallow foundation. Thus, MBR and MSR values are the indicators of to what extent a BSDF acts as a compound body. The more MBR and MSR values increase, the more a BSDF acts as a monolithic compound body-in other words. Fig. 4(9) illustrates that MBR values decrease as the depth increases. However, MSR values first tend to increase and then decrease with increasing depth. Fig. 4(11–12) shows that MBR and MSR values are much closer to one at relatively low and high widths. Moreover, as the aspect ratio increases, MBR and monolithic behavior decrease. BSDFs with lower aspect ratios

Fig. 5 a) monolith theory b) single element theory

(D/B) have MBR and MSR values closer to 1, and they act more like a monolithic-compound body. BSDFs with rough interfaces have MBR and MSR values closer to 1 and act more like a monolithic-compound body compared to the BSDFs with less rough interfaces.

2.3.3 Comparison of BSDFs and CPRFs
Randolph and Reul [20–22] have simulated various conventional piled raft foundation configurations to observe the load-settlement behavior. The parametric studies have shown that the optimized design of a CPRF depends on the subsoil conditions, the load and the pile configuration, and the load level. For CPRFs, the piles' position, the pile number, the pile length, the raft-soil stiffness ratio, and the load distribution on the raft might be varied. Therefore, there are infinite CPRF configurations to compare with BSDFs. For this reason, the concrete volume of deep foundations is to be taken as a comparison parameter to perform this comparison.

Efficiency is a situation in which a system or machine works well. This section aims to compare the performance of BSDFs and CPRFs by a numerical method to develop an efficiency concept. P% represents the "efficiency" which is equal to the percentile increase in load capacity of BSDF compared to CPRF with the same volume. Furthermore, the load capacity has been calculated corresponding to the 50 mm settlement of the foundation, which represents the allowable serviceability limit. For CPRFs, the pile space is selected as 3d since 2.5-3d pile spacing is recommended for the best performance in the literature. When the piles are placed close to each other, a reasonable assumption is that the stress transmitted by the piles to the soil will overlap, reducing the load-bearing capacity of the piles. The pile diameter of piles and box thickness are 1 m and 0.6 m, respectively. The sand and concrete surfaces were regarded as rough. Thus, no reduction was attributed to the resistance of the interface between sand and concrete.

As the aspect ratios of BSDFs increase, the efficiency surges and the highest efficiency value equals 11.3% for the BSDF configuration with the 5 m width and 1.5 m depth. However, other BSDF configurations show negative efficiency values that cause them not to be preferred over the representative CPRF. In addition to CPRFs with four piles, two additional CPRF configurations with 25 piles and 49 piles shown in Fig. 6 have also been compared to BSDFs with the same volume to observe the efficiency. Finally, 180 different models with different CPRF aspect ratios ranging from 1 to 4 and 3 distinct soil types
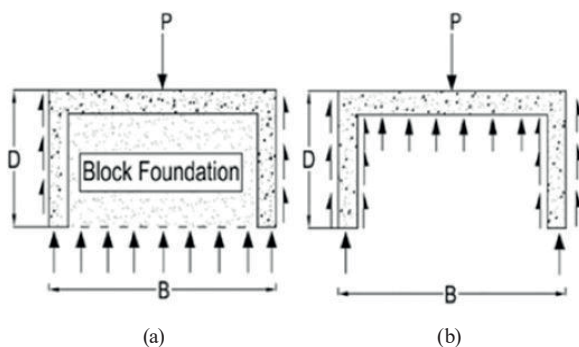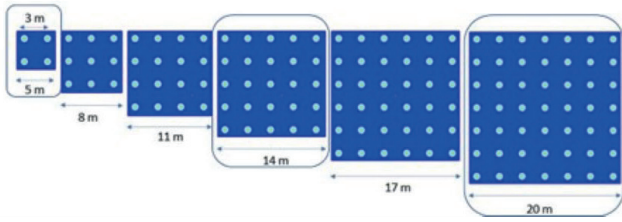
Fig. 6 Different CPRF configurations

for each are also simulated for comparison and interpretation. Figs. 7–9 show that the efficiency values (P%) of different BSDF configurations surge as the aspect ratio rises.

3 Experimental study
3.1 Experimental Setup
A laboratory testing setup comprised of a test tank with the dimensions of $100 \times 50 \times 65$ cm (length, width, depth) and a loading system has been used to determine the load-settlement behavior of BSDFs resting on sand for comparison with numerical analysis (Fig. 10). The loading system consists of a hydraulic jack, and loads are transferred to the foundation models through a loading rod.

Plates of aluminum with a thickness of 6 mm were used to model the walls and the rafts of BSDFs. The wall and raft elements were connected using screws. As for embedded foundations, an additional plate was mounted on the bottom part not to let soil penetrate inside. An LVDT transducer and an S-type load-cell were used to measure the displacements and load values on the footing.

Cerkezkoy sand was used in the experiment, and its index and strength properties, given in Table 2 were determined via laboratory tests. The test tank was divided into ten layers using 5 cm spaced lines on the plexiglass. At each layer, 10% of the required soil mass at the target relative density was poured, and the sand was compacted to the required volume.

The experimental process was conducted as (Fig. 11):
1. Throughout the experiment, in order to obtain the target relative density which is 35%, the 10% of the required soil mass was poured in each layer. When the required depth was reached, the box was placed on the soil.
2. The sand was poured into the box by obtaining the target relative density 35% and the raft plate was mounted by using screws.
3. After the placement of the BSDF, the soil was continued to be filled till the top level.
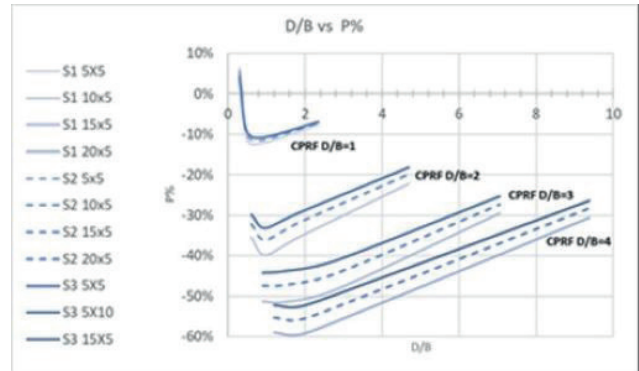4. The LVDT transducer was placed on the foundation's edge.

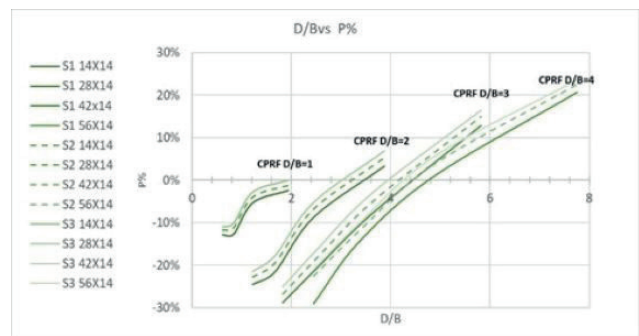**Fig. 7** The efficiency comparison of 5 m CPRF configurations

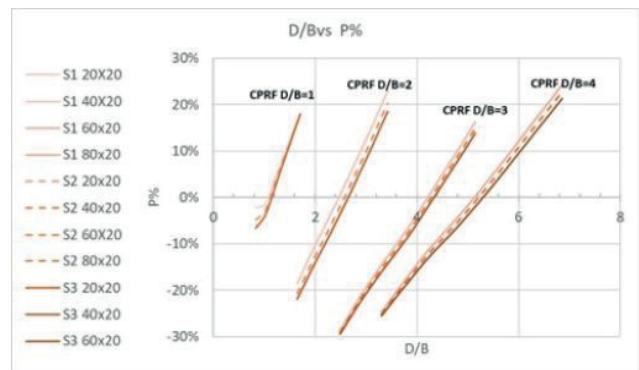**Fig. 8** The efficiency comparison of 14 m CPRF configurations

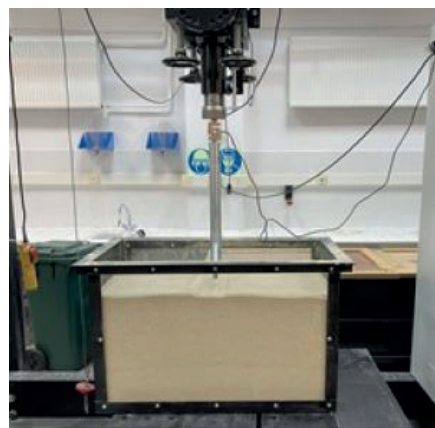**Fig. 9** The efficiency comparison of 20 m CPRF configurations

Fig. 10 Laboratory testing setup

Table 2 Index and strength properties of the Cerkezkoy Sand

Property	Value
Classification	SP
Median Particle Size (D50)	0.64
Coefficient of Uniformity (Cu)	2.37
Coefficient of Curvature (Cc)	0.93
Specific Gravity (Gs)	2.62
Maximum Void Ratio (emax)	0.83
Minimum Void Ratio (emin)	0.5
Average Sphericity (Save)	0.56
Average Roundness (Rave)	0.749
Critical state friction angle (φc)	33.04
Secant Modulus (E50) (Mpa)	16.3

Table 3 Dimensions of model foundation

Model Foundation	Depth (D) (cm)	Width (B) (cm)
BSDF 20 × 10	20	10
Embedded 20 × 10	20	10
BSDF 10 × 10	10	10
Embedded 10 × 10	10	10

Fig. 12 Numerically and experimentally obtained load - settlement plots

Fig. 12 displays the numerically and experimentally obtained load and settlement plots for BSDFs and their embedded counterparts. In all cases, the bearing capacity was calculated according to the 10% of the width which was 10 mm. Table 4 shows that there is a reasonable agreement between the numerical and experimental load-settlement behaviors.

3.3 Monolithic behavior

As mentioned before, MBR stands for the "monolithic bearing ratio" which is equal to the ratio of bearing capacity of BSDF to the bearing capacity of the representative embedded foundation. Thus, MBR indicates to what extent a BSDF acts as a compound body and the closer MBR gets to 1, the more a BSDF acts as a monolithic compound body. Table 5 demonstrates that the numerically and experimentally obtained load capacity values for embedded foundations compared to BSDFs are higher. As aspect ratios increase, MBR values for both numerical and experimental cases decrease. A similar trend has been observed for numerical analysis in Section 2.

4 Conclusions

The main objective of this study was to assess the load-settlement and monolithic behavior of BSDFs. Furthermore, a comparison between the load-settlement behavior of BSDFs and CPRFs with the same volume has been made to investigate the efficiency of BSDFs. Physical model
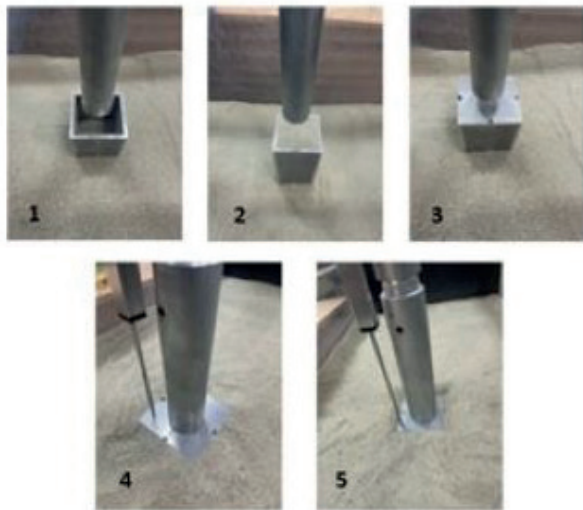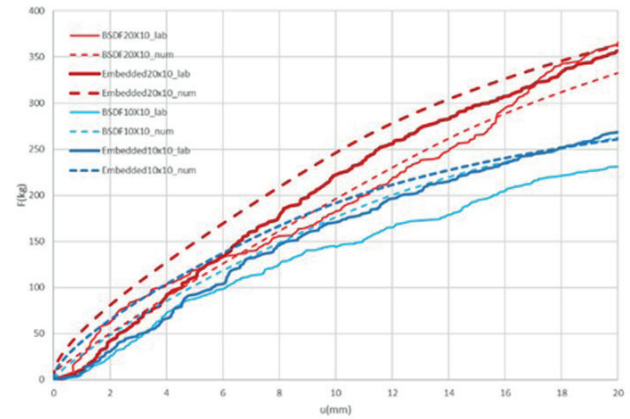

Fig. 11 The Experimental process

5. The BSDF was loaded at a constant rate of 10 mm/min until the displacement of 20 mm. Load-displacement values were recorded by LabView software to be assessed.

3.2 Load-settlement behavior

After conducting load-settlement tests on model foundations shown in Table 3, a numerical analysis was performed using Plaxis 3D to verify the test results and infer the performance of parametric studies. In this analysis, the parameters of HSs model for the relative density of 35% were calculated using formulas in Table 1. However, unit weight, Young's modulus, friction angle and dilation angle parameters of HSs model were revised by considering the laboratory test values in Table 2. The surfaces between the sand and the aluminum plates were regarded as smooth and a strength reduction factor (R_{int}) of 0.5 was selected to represent the soil-structure interaction of BSDFs.

Table 4 Experimentally and numerically obtained load capacity values

Model Foundation	Depth (D) (cm)	Width (B) (cm)	Load Capacity (kg)		Difference
			Experimental	Numerical	
BSDF 20 × 10	20	10	182.49	196.07	7%
Embedded 20 × 10	20	10	222.34	246.16	10%
BSDF 10 × 10	10	10	144.14	176.51	18%
Embedded 10 × 10	10	10	170.4	191.54	11%

Table 5 Experimentally and numerically obtained MBR values

Model Foundation	D/B	Load Capacity (kg)		MBR	
		Experimental	Numerical	Experimental	Numerical
BSDF 20 × 10	2	182.49	196.07	0.82	0.80
Embedded 20 × 10	2	222.34	246.16		
BSDF 10 × 10	1	146.14	176.51	0.86	0.92
Embedded 10 × 10	1	170.4	191.54		

tests were carried out on BSDFs and embedded foundation counterparts to validate the numerical approach presented in this study, and it turned out to be a reasonable agreement.

As a rule, the bearing capacity could be improved and settlements could be reduced by using BSDFs, but it should be realized that the load-settlement behavior depends on the geometry of BSDFs, soil conditions, surface roughness, load level, and load configuration. As the aspect ratio (D/B) increases, Bearing Capacity Ratio (BCR) increases and the Settlement Reduction Ratio (SRR) decreases. BSDFs with different aspect ratios in loose sand have achieved better results regarding bearing capacity and settlement than those at medium or high relative density sands. The reason behind this phenomenon might be explained as more space is available to increase the shear strength of loose soil than dense soil. Namely, the bearing capacity ratio is higher in loose soil because the displacement to mobilize the strength in dense soil is not enough compared to that in loose soil. The bearing capacity and settlement reduction improvement increase with the increasing surface roughness. This fact was attributed to the diaphragm walls that do not sufficiently contribute to load transition. Hence, a significant part of the uniaxial loads is assigned to the tip level, resulting in a decreasing bearing capacity rate.

Monolithic Bearing Ratio (MBR) and Monolithic Settlement Ratio (MSR) values are the indicators of the monolithic-compound body behavior of BSDFs. It can be said that BSDFs with rough interfaces and lower aspect ratios (D/B) have MBR and MSR values closer to 1 and they act more like a monolithic-compound body, compared to the BSDFs with less rough interfaces and higher aspect ratios (D/B). Although not as obvious as load-settlement behavior, monolithic behavior is also impacted by the relative density of the sand. Denser sands show more monolithic behavior at relatively lower aspect ratios. While the foundation and drifting soil go downward, the more constrained soil at the bottom part of the foundation than the soil near the top part of the foundation leads to soil arching. The increase in this arching effect is more pronounced for BSDFs with low aspect ratios.

By comparing BSDFs with CPRFs of the same volume, the parametric study revealed that the efficiency of BSDFs mainly depends on the geometry of BSDFs. Hence, a generalization of the efficiency of BSDFs for all possible cases in practice is not possible. Nevertheless, key outcomes of this parametric study can be quite helpful in the beginning of a project to decide which deep foundation configuration options should be considered. BSDFs with relatively small geometry such as 5 m width have positive efficiency values at smaller aspect ratios when compared with CPRFs with an aspect ratio of 1. CPRFs with higher aspect ratios are inclined to have higher load capacity than BSDFs with the same volume. As the width of the foundation increases, BSDFs are more inclined to have positive efficiency values at increasing aspect ratios. For example, A BSDF with a box configuration of 14 m width and 96 m depth under a 20 x 20 raft has the highest efficiency of 35% compared to a CPRF with an aspect ratio of 4 under the same raft. For a given aspect ratio, BSDFs over denser soil are more prone to have higher efficiency values for widths of 5 and 14 meters. However, BSDFs with 20 m width have higher efficiency values at relatively loose sands.

It can be concluded that Box-shaped Deep Foundations could be an alternative to Conventional Piled Raft Foundations in several cases, considering the efficiency concept presented in this study. Moreover, their resistance to scouring effects and allowance to be utilized as retaining structures could be other appealing features of BSDFs.

References

[1] Brandl, H. "Deep Box-foundations with Piles and Diaphragm Walls on Weak Soils", In: Proceedings of the 9th Southeast Asian Geotechnical Conference, Vol. II, 6 Shallow and Deep Foundations, Bangkok, Thailand, 1987, pp. 6–15.

[2] Hofmann, R. "Trag- und Setzungsverhalten von Pfahlkästen" (Bearing and settlement behavior of pile boxes), PhD Thesis, TU-Wien, 2001.

[3] Brandl, H. "Conventional and Box-shaped Piled Rafts", In: Proceedings of the 15th International Conference on Soil Mechanics and Geotechnical Engineering (ICSMGE), Istanbul, Turkiye, 2001, pp. 1099–1108.

[4] Wen, H., Cheng, Q., Meng, F., Chen, X. "Diaphragm wall-soil-cap interaction in rectangular closed diaphragm wall bridge foundations", Frontiers of Architecture and Civil Engineering in China, 3, pp. 93–100, 2009.
https://doi.org/10.1007/s11709-009-0015-4

[5] Cheng, Q., Wu, J., Song, Z., Wen, H. "The behavior of a rectangular closed diaphragm wall when used as a bridge foundation", Frontiers of Structural and Civil Engineering, 6, pp. 398–420, 2012.
https://doi.org/10.1007/s11709-012-0175-5

[6] Wu, J., El Naggar, M. H., Cheng, Q., Wen, H., Li, Y., Zang, J., "Iterative load transfer procedure for settlement evaluation of lattice-shaped diaphragm walls in multilayered soil", Computers and Geotechnics, 120, 103409, 2020.
https://doi.org/10.1016/j.compgeo.2019.103409

[7] Martínez-Galván, S. A., Romo, M. P. "Assessment of an alternative to deep foundations in compressible clays: the structural cell foundation", Frontiers of Structural and Civil Engineering, 12, pp. 67–80, 2018.
https://doi.org/10.1007/s11709-017-0399-5

[8] Byrne, B. W., Houlsby, G. T. "Drained Behaviour of Suction Caisson Foundations on Very Dense Sand", In: Offshore Technology Conference, Houston, TX, USA, 1999, Paper no. OTC-10994-MS. ISBN: 978-1-55563-247-2
https://doi.org/10.4043/10994-MS

[9] Park, J.-S., Park, D., Yoo, J. K. "Vertical Bearing Capacity of Bucket Foundations in Sand", Ocean Engineering, 121, pp. 453–461, 2016.
https://doi.org/10.1016/j.oceaneng.2016.05.056

[10] Al-Aghbari, M. Y., Mohamedzein Y. E.-A. "The use of skirts to improve the performance of a footing in sand", International Journal of Geotechnical Engineering, 14(2), pp. 134–141, 2020.
https://doi.org/10.1080/19386362.2018.1429702

[11] Eid, H. T. "Bearing Capacity and Settlement of Skirted Shallow Foundations on Sand", International Journal of Geomechanics, 13(5), pp. 645–652, 2013.
https://doi.org/10.1061/(ASCE)GM.1943-5622.0000237

[12] Gnananandarao, T., Dutta, R. K., Khatri, V. N. "Model Studies of Plus and Double Dox Shaped Skirted Footings resting on sand", International Journal of Geo-Engineering, 11, 2, 2020.
https://doi.org/10.1063/1.5026698

[13] Plaxis "Material Models Manual, 3D 2023.1", Bentley, 2020. [online] Available: https://communities.bentley.com/products/geotech-analysis/w/wiki/46137/manuals---plaxis

[14] Brinkgreve, R. B. J., Engin, E., Engin, H. K. "Validation of Empirical Formulas to Derive Model Parameters for Sands", In: Proceedings of 7th European Conference Numerical Methods in Geotechnical Engineering, Trondheim, Norway, 2010, pp. 137–142. ISBN: 9780415592390

[15] Obrzud, R. F., Truty, A. "The Hardening Soil Model – A Practical Guidebook", Zace Services Ltd, Lausanne, Switzerland, Rep. ZSoil.PC100701, 2020.

[16] Potts, D. M., Zdravković, L. "Finite element analysis in geotechnical engineering, Theory", Thomas Telford, 1999. ISBN: 0 7277 2753 2

[17] Vesić, A. S. "Analysis of Ultimate Loads of Shallow Foundations", Journal of Soil Mechanics and Foundation Engineering Division, 99(1), pp. 45–73, 1973.
https://doi.org/10.1061/JSFEAQ.0001846

[18] Van Langen, H., Vermeer, P. A. "Interface elements for singular plasticity points", International Journal for Numerical and Analytical Methods in Geomechanics, 15(5), pp. 301–315, 1991.
https://doi.org/10.1002/nag.1610150502

[19] Potyondy, J. G. "Skin friction between various soils and construction materials", Géotechnique, 11(4), pp. 339–353, 1961.
https://doi.org/10.1680/geot.1961.11.4.339

[20] Randolph, M. F. "Design Methods for Pile Groups and Piled Rafts", In: Proceedings of 13th International Conference on Soil Mechanics and Foundation Engineering, New Delhi, India, 1994, pp. 61–82. ISBN: 9054103701

[21] Reul, O., Randolph, M. F. "Piled Rafts in Overconsolidated Clay: Comparison of in situ Measurements and Numerical Analyses", Geotechnique, 53(3), pp. 301–315, 2003.
https://doi.org/10.1680/geot.2003.53.3.301

[22] Reul, O. "Numerical Study of the Bearing Behavior of Piled Rafts", International Journal of Geomechanics, 4(2), pp. 59–68, 2004.
https://doi.org/10.1061/(ASCE)1532-3641(2004)4:2(59)